

Investigating Into the Effects of Bore Irregularities on the Hydrodynamic Performance Journal Bearing Using Response Surface Methodology

Sushanta Kumar Pradhan^a, Anand Gupta^b, Prakash Chandra Mishra^{a,*}

^aDepartment of Mechanical Engineering, Veer Surendra Sai University of Technology, Burla, India-768018,

^bDepartment of Mechanical Engineering, Indira Gandhi Institute of Technology, Sarang, India-759146.


Keywords:

Journal bearing
Non-circularity
Roughness coefficient
Load bearing capacity
Friction
Flow-in
Response surface methodology
Desirability

ABSTRACT

The current research is focused on investigating the influence of bearing irregularities like eccentricities (ϵ), non-circularities (G), L/D ratio (β), surface roughness coefficient (Y) on hydrodynamic performance of journal bearing such as load bearing capacity, friction force, lubricating oil flow. The performance is evaluated through finite difference method technique implementing a Newton-Raphson method of error convergence. The simulation outputs were than designed using an optimization tool entitled as Design of Experiment (DoE) on basis of response surface methodology (RSM). The outputs of RSM models were meant to forecast the response parameters like, load bearing capacity, friction force, flow of lubricant and further required to identify the noticeable interdependencies within the input parameters while evaluating the lubrication performance. The optimization of the bearing irregularities is done considering desirability approach of the response surface methodology in identifying proper combination of parameters.

* Corresponding author:

Prakash Chandra Mishra 
E-mail: pcmishra_me@vssut.ac.in

Received: 3 January 2023

Revised: 9 February 2023

Accepted: 21 March 2023

© 2023 Published by Faculty of Engineering

1. INTRODUCTION

Journal bearing operates in hydrodynamic regime of lubrication. Its performance is largely influenced by various geometrical and operational parameters. Such parameters have highly non-linear effects on various performance characteristics. In the real practice, journal bearing system possess many irregularities associated with its geometric and operational level. Eccentricities, non-circularity, misalignment, roughness pattern on bearing and

journal surface are to name a few. In earlier research initiatives, Crosby [1] and Mishra et al. [2] investigated the influence of bore non-circularity upon the hydrodynamic characteristics of irregular journal bearing and predicted the presence of bore ellipticity up to ($G=1.0$) found to be favorable for journal bearing stability. Literatures also reported the effect of roughness pattern and its effect on the journal bearing for both circular [3,4] and non-circular [5] bore configurations. Rotating fluid film develops heat out of fluid shear of intermediate

lubricating oil layers [6]. Hence, operational irregularities like misalignment also have profound effect on bearing performance. Mishra et al. [7] studied a misaligned non-circular bore journal bearing with heat generating and non-Newtonian effects. From this study, it is realized that there are numerous parameters with their influence, makes the journal bearing analysis more complex, which requires the optimization techniques to understand most influential and least influential parameters. Mishra et al. [8] applied Taguchi Grey optimization technique Grey-Fuzzy hybrid [9] to identify most favorable condition for bearing performance. Application of Artificial Neural Network is also found [10] in journal bearing performance training, testing and validation.

In this context, application of Response Surface Methodology (RSM) will be a new approach. It can identify influence of multiple parameters in single performance output. Such approach has already applied to other engineering problems. Pandian et al. [11] studied a twin cylinder compression engine to analyse the effect of injection system parameters on power output and emission characteristics while running in pongamia biodiesel–diesel blend considering RSM. Ahemad et al. [12] utilized the RSM to study oil film friction of a fluid film bearing and compared the predicted and observed parameters with good agreement. Lee et al. [13] further considered the response surface methodology for a HSDI diesel engine using common rail injection system. Zang et al. [14] developed a simulation technique for a constant load based RSM to optimize lubrication properties calculated from simultaneous solution of Navier-Stokes equation and elastic deformation equation. Response surface methodology is also applied for fault diagnosis of rotor bearing, Kankar et al. [15] and Mishra et al. [16], where the dynamic responses are predicted.

In multivariate journal bearing problem, the application of non-linear technique like design of experiment (DoE), Grey-fuzzy and neural network type decision making techniques are more appropriate for exploring the combined influence of input data. DoE out of those is most suitable and less costly method to estimate the single as well as interlinked effects of input parameters on output responses. There are limited investigations carried out on the use of DoE on the journal bearing performance analysis, the study on combined effect

between bore irregularities and bearing performance parameters are not discussed and indicates a scope for such research. The primary goal of our research is to investigate the independent and interlinked influences of bearing input parameters related to the performance characteristics of journal bearing considering ellipticity, non-circularity, roughness coefficient, L/D ratio as input parameters of the model to discuss the response parameters like load bearing capacity, friction force and oil flow.

2. THEORITICAL FORMULATION

Bore irregularities

The bearing parameters like eccentricity ratio (defined as ratio of centre distance between journal and sleeve, $\epsilon_{0.3-0.8}$), while non-circularity (G) is defined as the degree of ovality/ ellipticity considered in the range of (0.0-3.0) derived by Mishra et al. [5]. Here, roughness coefficient(Y) is defined as half total range of random film thickness variable defined by Christensen and Tonder [4] and taken in the range of (0-0.3).

Rough elliptic bore film profile

The film thickness expression for a non-circular bore is given in Eq. (1) as per Mishra et al. [7]

$$H = 1 + G \cos^2 \theta + \epsilon \cos \theta \quad (1)$$

Governing Equation

The Reynolds equation for a journal bearing including irregular roughness as per Christensen and Tonder [3-4] is modified with expectancy operators $\zeta(x)$ is:

$$\frac{\partial}{\partial x} \zeta \left(H^3 \frac{\partial P}{\partial x} \right) + \frac{\partial}{\partial z} \zeta \left(H^3 \frac{\partial P}{\partial z} \right) = 6\eta u \frac{\partial}{\partial x} \zeta(H) \quad (2)$$

Where,

$$\zeta(x) = \int_{-\infty}^{\infty} x f(x) dx \quad (3)$$

is the Expectancy operator.

The $f(x)$ is stochastic function, which represents probability distribution of variables. To include the expectancy operators, Eq. (4) can otherwise be presented as per Mishra et al. [7] as follows:

$$\frac{\partial}{\partial x} \left(\frac{\partial P}{\partial x} g_1(H) \right) + \frac{\partial}{\partial z} \left(\frac{\partial P}{\partial z} g_2(H) \right) = 6\eta u \frac{\partial}{\partial x} g_3(H) \quad (4)$$

The solution of Reynold’s equation carried out using finite difference method with central difference technique [5] with error convergence through effective influence Newton-Raphson method with a minimum converging error of 10^{-5} .

Solution of the model

The Reynolds second order partial differential equation is solved using finite difference technique as per Mishra et al. [7] as a boundary value problem with mass-conserving algorithm of Elrod. The method involves a switch function, $g(\theta_c)$, that plays an importance role in the cavitation index, where $g(\theta_c) = 1$ for $p \geq p_{cav}$ and $\rho \geq \rho_{cav}$, while $g(\theta_c) = 0$ for $p \leq p_{cav}$ and $\rho \leq \rho_{cav}$. The numerical technique involves the low-relaxation effective influence Newton-Raphson iterative method for pressure error convergence. In the zone of cavitation, the liquid mass content is controlled by ρ_{cav} , θ_c , and h (as $\rho_{cav} \cdot \theta_c \cdot h$), where h is the film thickness. This variable is the dimensionless density, which is the fraction of lubricant content in the cavitation zone. Here, $(1-\theta_c)$ is the cavity void fraction. When a solution to θ_c is obtained, the pressure profile can be reconstructed. The unwrapped bearing surface is discretized to form a grid of (100×25) , which gives a square grid element for the stable hydrodynamic pressure [18] of film geometry.

Load carrying capacity

The load bearing capacity of elliptic bore bearing is evaluated using Simpson’s rule, and is given in Eq. (5). Mishra et al. [2] used this equation to evaluate the load bearing capacity of a non-circular journal bearing.

$$W^* = \frac{\Delta\theta\Delta z}{9} \int_{\theta_0}^{\theta_m} \int_{z_0}^{z_n} P(\theta, z) \partial\theta\partial z \quad (5)$$

Fig. 1 (a) shows the load ratio (W_e/W_c) response to the non-circularity ratio (G_i/G_o) for a short journal bearing. Load ratio increases with elevating non-circularity till ($G=0.5$) for medium and higher order eccentricity. Due to presence of non-circularity at lower eccentricity ($\epsilon = 0.3$) till ($G= 1.0$), bearing load ratio (W_e/W_c) has an increase in trend.

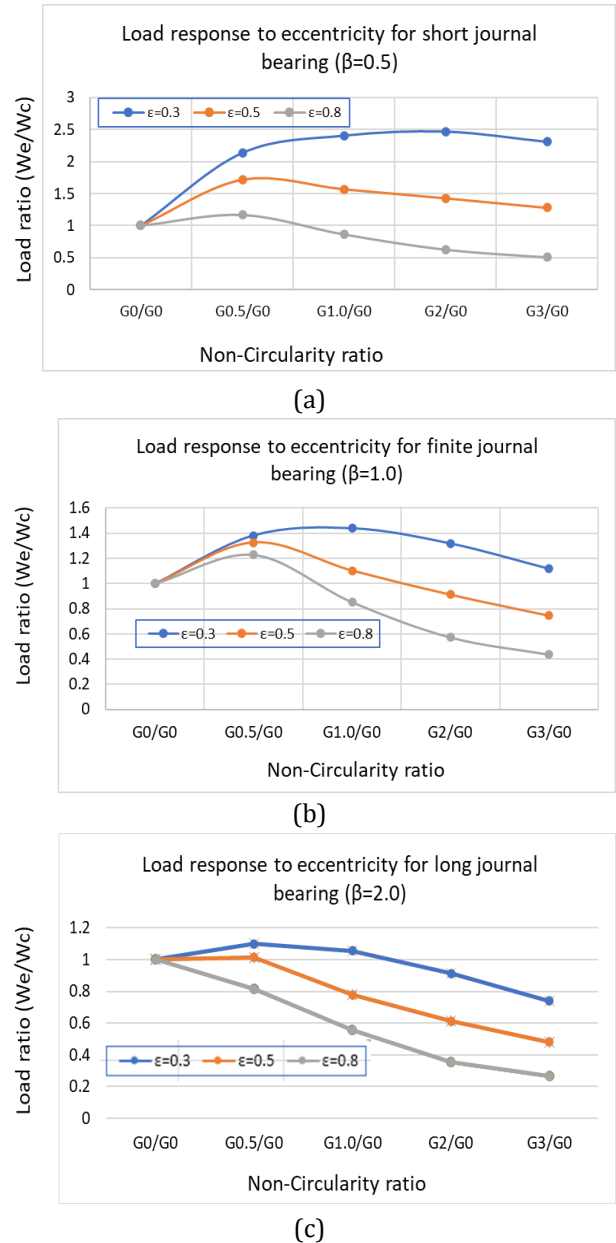


Fig. 1. (a) Load response to eccentricity for short journal bearing, (b) Load response to eccentricity for finite journal bearing, (c) Load response to eccentricity for long journal bearing.

Fig. 1 (b) shows the load ratio (W_e/W_c) response to the non-circularity ratio (G_i/G_o) for a finite journal bearing. Compared to short journal bearing, finite journal bearing has less load bearing capacity ratio, which may be due to simultaneous effect of eccentricity and non-circularity causes this alteration. With increasing eccentricity, non-circular bearing load ratio (W_e/W_c) decreases. Fig. 1 (c) shows the load ratio response to non-circularity ratio (G_i/G_o) for long journal bearing ($\beta=2.0$). Long journal bearing with non-circularity more than ($G=0.5$) is not recommended for load carrying capacity point of view.

Friction force of the bearing

The stress developed due to lubricant shear in hydrodynamic case is given in Eq. (6).

$$\tau = \frac{\eta U}{h} - \frac{h}{2} \frac{\partial p}{\partial x} \tag{6}$$

Such shear stress in the mixed regime for the pressure zone and the cavitation zone is presented in Eq. (7) and Eq. (8) respectively as per Christensen and Tonder [4].

$$\bar{\tau} = \frac{1}{2} \frac{\partial p}{\partial x} \mathcal{G}_3(h) + \eta u [\mathcal{G}_4(h) - \mathcal{G}_5(h)] \tag{7}$$

in pressure zone

$$\bar{\tau} = \eta u [\mathcal{G}_4(h) - \mathcal{G}_5(h)] \tag{8}$$

in cavitation zone.

Further, the fluid friction is the shear stress integrated on the contact surface area of bearing bore and presented in Eq. (9):

$$F = \iint \tau dx dy \tag{9}$$

Fig. 2 (a) shows the non-dimensional friction response to roughness coefficient (Y) for non-circularity (G=0.5). Roughness up to (Y=0.1) enhances the friction force. At particular roughness coefficient, for higher eccentricities, the friction force is more. Highest non-dimensional friction force of 75 occurs at roughness coefficient value (Y=0.1). Fig. 2 (b) shows the friction response to the roughness coefficients (Y= 0,0.1,0.2 &0.3). At same roughness coefficient, bearing with higher non-circularity has more friction force due to fluid layer interaction. At the non-circularity of (G=1.0), the highest value of non-dimensional friction force is 142 at roughness coefficient of (Y=0.1).

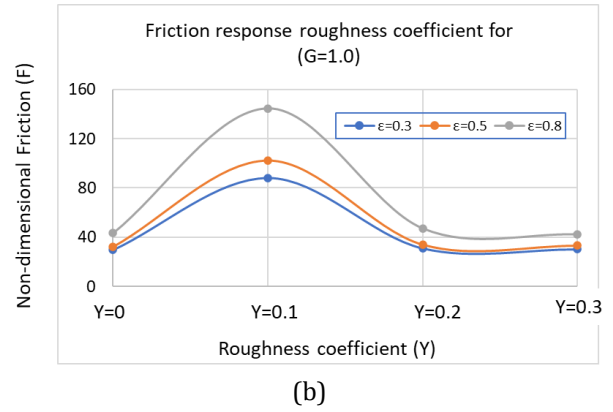
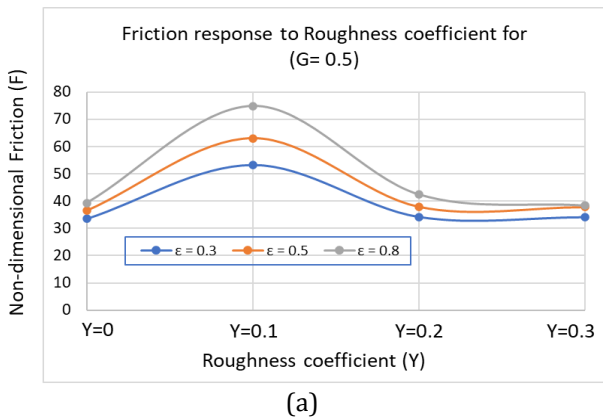


Fig. 2. (a) Friction response to roughness coefficient for non-circularity (G=0.5), (b) Friction response to roughness coefficient for non-circularity (G =1.0).

Flow-in and side leakage

The lubricant oil flow rate for smooth case was evaluated with consideration of Eq. (10).

$$q_{\theta}^* = \frac{Uh}{2} - \frac{h}{2} \frac{\partial p}{\partial x} \tag{10}$$

While in case rough bearing the flow intensity is given in Eq. (11) per Christensen and Tonder [4].

$$q_{\theta}^* = \frac{u}{2} \mathcal{G}_3(h) - \frac{1}{12\eta} \frac{\partial p}{\partial x} \mathcal{G}_1(h) \tag{11}$$

And,

The total flow-in circumferential direction is given in Eq. (12).

$$Q_{in} = \iint q_{\theta}^* dx dy \tag{12}$$

The side leakage rate in journal bearing conjunction for smooth case is evaluated by using Eq. (13).

$$q_s^* = - \left(\frac{h^3}{2} \right) \frac{\partial p}{\partial z} \tag{13}$$

While for rough bearing, side leakage is given in Eq. (14) per Christensen and Tonder [4].

$$q_s^* = - \frac{1}{12\eta} \frac{\partial p}{\partial y} \mathcal{G}_2(h) \tag{14}$$

And,

The total side leakage along the bearing length is given in Eq. (15)

$$Q_s = \iint q_s^* dx dy \tag{15}$$

Fig. 3 (a) and Fig. 3 (b) show the flow-in (Q_{in}) response to roughness coefficient (Y) for bore non-circularity of $G=0.5$ and $G=1.0$ respectively for a finite width journal bearing. With increasing non-circularity, the flow-in to the bearing conjunction enhances. There is an increasing trend of lubricant flow till roughness coefficient of ($Y=0.1$).

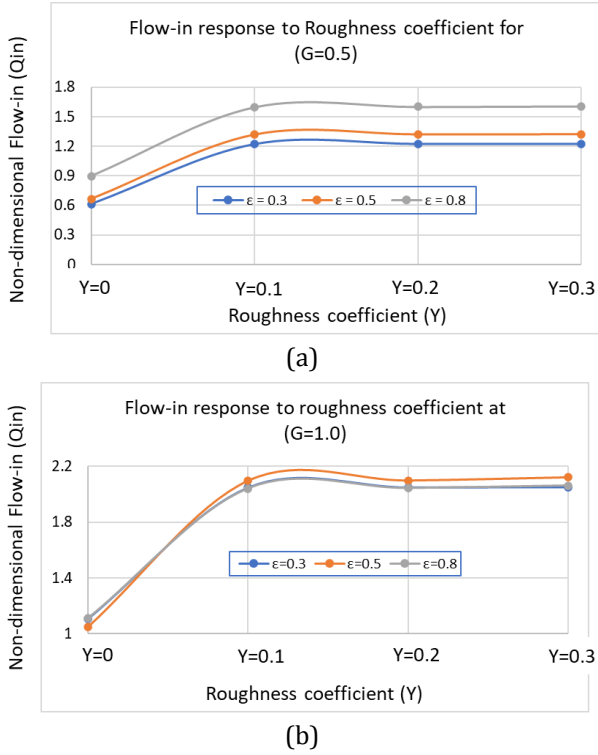
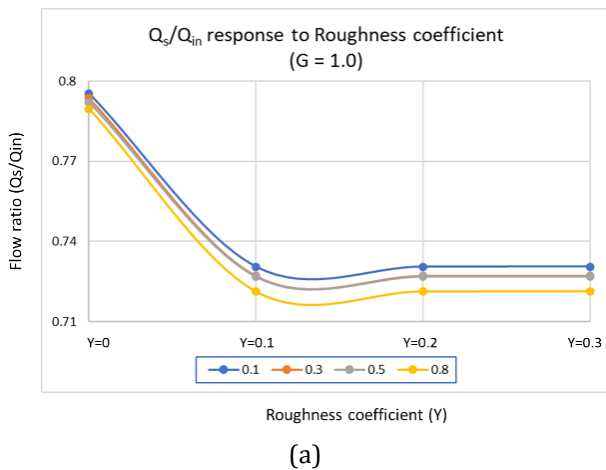
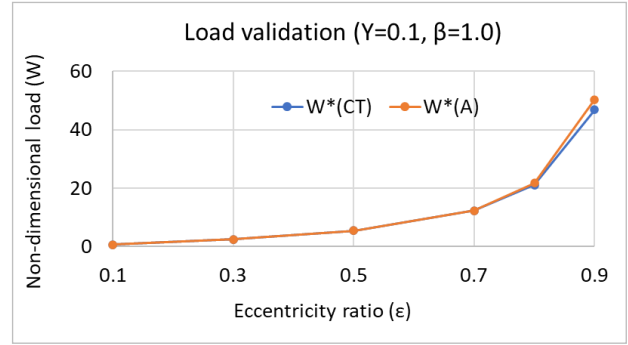


Fig. 3. (a) Flow-in response to roughness coefficient for non-circularity ($G = 0.5$), (b) Flow-in response to roughness coefficient for non-circularity ($G = 1.0$).

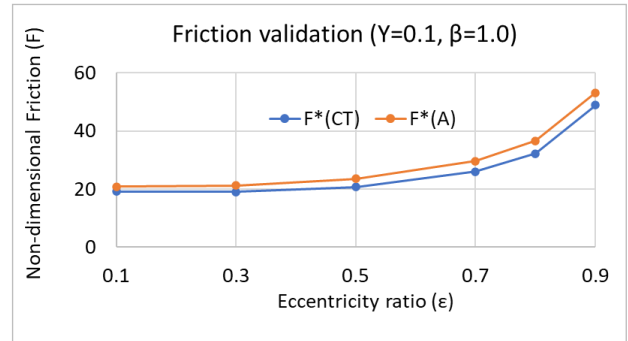
Fig. 4 (a) shows the oil flow ratio (Q_s/Q_{in}) into the bearing. With increasing roughness coefficient, the flow ratio decreases until ($Y=0.2$). There after it remains almost constant till ($Y=0.3$).



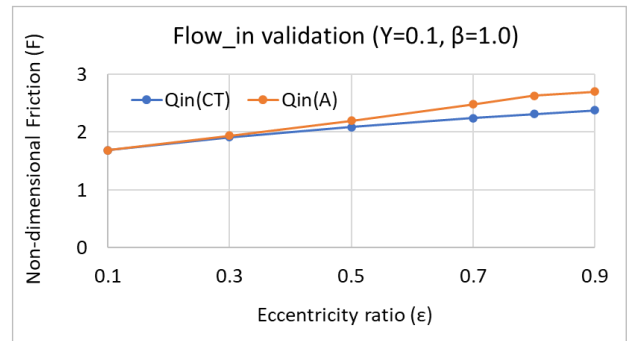
(a)



(b1)



(b2)



(b3)

Fig. 4. (a) Flow ratio (Q_s/Q_{in}) response to roughness coefficient for non-circularity ($G = 1.0$), (b) Validation of performance parameters with Christensen and Tonder [4].

Fig. 4 (b) shows the validation of the performance with Christensen and Tonder [4] and found to be matching with less than 3% error.

3. RESULTS AND DISCUSSION OF RSM

Response surface methodology for irregular bearing analysis

The response parameters related to rough non-circular bore journal bearing characteristics modelling are introduced in surface response methodology. The RSM model and investigations on the experiment consists of the following steps:

- The initial step of RSM here is to select the input parameters that affect hydrodynamic performance of the journal bearing. In current analysis, the eccentricities (ϵ), L/D ratio (β), non-circularity (G), roughness coefficient (Y) were considered as the RSM input data.
- Then, eccentricities (ϵ) were varied at three levels from 0.3 to 0.5 and from 0.5 to 0.8. The L/D ratio (β) too changed in three steps from 0.5 to 1.0 and from 1.0 to 2.0. The non-circularity (G) also varied at three levels from 0.5 to 1.0 and from 1.0 to 2.0. Finally, the roughness coefficient (Y) also varied at three levels from 0.1 to 0.2 and from 0.2 to 0.3. the limitations of input parameters are were set on basis of permissible limits of individual parameters. Extremely low and high values are not included, which is the limitation of this study.
- The benefits of the DoEs here are to estimate the hydrodynamic outputs of journal bearing for whole range of input parameters involving least number of experiments. Here, the matrix for design is considered taking into account the fractional factorial design of RSM computed using simulation tool like "Design expert" version 7.1.5 of Stat ease, US, that contains 29 simulation runs that is given in table 2.
- According to the order of run, the simulations were performed on the elliptic bore journal bearing and amended in the response column.
- The coefficients were computed using multiple regression analysis. The equations thus generated were utilized to forecast the responses. Subsequently, the statistically important technique is considered for the interlinking between the simulation parameters, after which multiple responses were generated.
- At last, the optimum value of each the bearing performance parameter was acquired considering the desirability method of RSM.

Desirability approach of bearing performance monitoring

The problems associated with every system can yield multiple responses need optimization for decision making on favourable and unfavourable outcomes. The limitation of optimization problem is overlying of counter plot of each response, which necessitates desirability assessment. Such

assessment is easy to use even in common software setup and flexible in measuring parameters considering significance of single response. For the current analysis, RSM-based desirability technique is considered for optimizing bearing input parameters such as (eccentricities (ϵ), non-circularities (G), L/D ratio (β), roughness coefficient (Y)) for the output performances (i.e., load bearing capacity (W), friction force (F) and lubricant flow both into (Q_{in}) and out of (Q_s) bearing). The optimization process is performed implementing Design Expert software, in which individual response is interpreted to a dimensionless desirability value (d) which varies between ($0 < d < 1$); where, $d=0$ denotes the response is fully unacceptable, whereas for $d=1$, indicates the response is more desirable. Here, the objective of each response is either to maximize, minimize, or target, in the limit and/or equal to deciding the quality of the problem. Here, the desirability of individual response is estimated using equations pertaining to the objective of each response [11] as given in Eq. (16).

In least valued objective, $d_i=1$ when $Y_i \leq Low_i$; $d_i=0$ when $Y_i \geq High_i$; and

$$d_i = \left(\frac{High_i - Y_i}{High_i - Low_i} \right)^{w_i} \tag{16}$$

when $Low_i < Y_i < High_i$

For an objective of highest value, $d_i=0$ when $Y_i \leq Low_i$; $d_i = 1$ when $Y_i \geq High_i$ as in Eq. (17)

And

$$d_i = \left(\frac{Y_i - Low_i}{High_i - Low_i} \right)^{w_i} \tag{17}$$

where $Low_i < Y_i < High_i$

In case of targeted goal, $d_i=0$, when $Y_i < Low_i$; $Y_i > High$ as in Eq. (18).

$$d_i = \left(\frac{Y_i - Low_i}{T_i - Low_i} \right)^{w_{ri}} \tag{18}$$

where $Low_i < Y_i < T_i$

$$d_i = \left(\frac{Y_i - High_i}{T_i - High_i} \right)^{w_{ri}} \tag{19}$$

where $T_i < Y_i < High_i$

As given in Eq. (19)

For the goal within the limit, $d_i = 1$ where $Low_i < Y_i < High_i$, and $d_i=0$; elsewhere.

$$D = \left(\prod_{i=1}^n d_i^{w_i} \right)^{1/\sum w_i} \tag{20}$$

In this case, ‘i’ is the response, ‘ Y_i ’ is the level of response, ‘Low’ means bottom limit of response. ‘High’ indicates the higher side of response. ‘T’ is the targeted value of the response, whereas ‘wt’ to be the weight of the response [11]. The trace of the desirability function supposed to be different for individual response in the weight field. Where, weights to be induced to depict higher significance on lower / upper bound. Weights were changed from 0.1 to 10; a weight greater than 1 has more significance on the goal, while weighs less than 1 shows less significance. When the weight value is 1, desirability function responds in a linear trend. Solution of multi-response optimization implementing desirability technique requires a method of multi-responses integrated to dimensionless performance parameters measurement. It is defined as net desirability function, D, ($0 \leq D \leq 1$) and is evaluated using Eq. (20)

For the net desirability function (D), individual response is constrained as an important relation to the other responses. Significance ranges from the least important grade of 1, denoted as (+), whereas the most significant grade of 5, denoted as (+++++). An elevated value of D denotes the more desirable and outstanding function of the journal bearing operation that is adjudged as the optimal solution [11]. The optimized parameters are selected out of individual desired functions(d) which maximizes D. Table 1 presents the details of input parameters required for the RSM simulation.

Table 1. Description of input parameters.

| Sl. no | Independent variables | Unit | Low level | High level |
|--------|-----------------------|------|-----------|------------|
| 1 | ϵ | -- | 0.3 | 0.8 |
| 2 | β | -- | 0.5 | 2 |
| 3 | G | -- | 0.5 | 2 |
| 4 | Y | -- | 0.1 | 0.3 |

To estimate the collective outcomes of input responses, the DoE (Design of Experiment) is formulated and presented in table 2.

Table 2. Design of Experiment (DoE).

| Run | Factor 1 A: ϵ | Factor 2 B: β | Factor 3 C: G | Factor 4 D: Y | Response 1 W_s | Response 2 W_R | Response 3 F_s | Response 4 F_R | Response 5 Q_s | Response 6 Q_R |
|-----|---------------------------|------------------------|------------------|------------------|---------------------|---------------------|---------------------|---------------------|---------------------|---------------------|
| 1 | 0.8 | 1 | 1 | 0.1 | 16.45 | 19.55 | 144.67 | 43.33 | 2.04 | 1.12 |
| 2 | 0.3 | 1 | 0.5 | 0.2 | 5.53 | 4.54 | 34.21 | 33.17 | 1.22 | 1.99 |
| 3 | 0.8 | 0.5 | 1 | 0.2 | 12.96 | 9.27 | 43.38 | 42.16 | 4.21 | 8.17 |
| 4 | 0.5 | 0.5 | 0.5 | 0.2 | 6.53 | 3.56 | 37.14 | 38.32 | 2.66 | 6.11 |
| 5 | 0.5 | 2 | 0.5 | 0.2 | 12.24 | 10.46 | 38.23 | 41.56 | 0.52 | 2.32 |
| 6 | 0.5 | 1 | 1 | 0.2 | 7.48 | 5.43 | 34.04 | 38.52 | 2.11 | 3.19 |
| 7 | 0.5 | 0.5 | 2 | 0.2 | 4.58 | 7.82 | 38.34 | 43.12 | 4.27 | 6.73 |
| 8 | 0.5 | 1 | 0.5 | 0.1 | 9.29 | 6.76 | 62.96 | 73.78 | 1.76 | 2.34 |
| 9 | 0.3 | 1 | 2 | 0.2 | 4.85 | 3.96 | 28.56 | 34.98 | 3.14 | 3.54 |
| 10 | 0.8 | 1 | 0.5 | 0.2 | 23.83 | 22.52 | 42.39 | 51.78 | 1.6 | 1.78 |
| 11 | 0.5 | 0.5 | 1 | 0.3 | 5.63 | 3.46 | 32.71 | 40.76 | 4.27 | 5.03 |
| 12 | 0.5 | 2 | 2 | 0.2 | 6.76 | 5.45 | 31.34 | 35.47 | 1.22 | 1.34 |
| 13 | 0.8 | 2 | 1 | 0.2 | 17.6 | 13.56 | 48.01 | 54.32 | 0.87 | 0.93 |
| 14 | 0.8 | 1 | 1 | 0.3 | 16.7 | 14.89 | 42.3 | 46.34 | 2.05 | 2.13 |
| 15 | 0.5 | 1 | 0.5 | 0.3 | 8.98 | 7.68 | 37.75 | 39.54 | 2.10 | 2.23 |
| 16 | 0.5 | 1 | 1 | 0.2 | 9.17 | 8.24 | 34.04 | 38.52 | 2.11 | 3.19 |
| 17 | 0.5 | 0.5 | 1 | 0.1 | 5.63 | 4.54 | 102.67 | 106.4 | 4.26 | 4.35 |
| 18 | 0.5 | 1 | 1 | 0.2 | 7.48 | 5.43 | 34.04 | 38.52 | 2.12 | 3.19 |
| 19 | 0.5 | 1 | 1 | 0.2 | 7.48 | 5.43 | 34.04 | 38.52 | 2.11 | 3.18 |
| 20 | 0.3 | 0.5 | 1 | 0.2 | 5.77 | 4.57 | 30.57 | 34.42 | 4.15 | 4.68 |
| 21 | 0.5 | 1 | 2 | 0.1 | 5.94 | 4.67 | 124 | 129.5 | 2.134 | 3.41 |
| 22 | 0.5 | 1 | 2 | 0.3 | 5.51 | 4.77 | 36.34 | 39.42 | 2.43 | 2.58 |
| 23 | 0.3 | 1 | 1 | 0.1 | 5.81 | 4.77 | 88.09 | 92.34 | 2.05 | 2.44 |
| 24 | 0.5 | 2 | 1 | 0.1 | 8.47 | 6.77 | 102.83 | 104.4 | 4.36 | 4.38 |
| 25 | 0.3 | 2 | 1 | 0.2 | 6.54 | 5.36 | 31.1 | 35.3 | 0.88 | 0.93 |
| 26 | 0.5 | 2 | 1 | 0.3 | 8.26 | 6.42 | 30.38 | 32.41 | 0.83 | 0.92 |
| 27 | 0.8 | 1 | 2 | 0.2 | 10.55 | 8.34 | 49.3 | 53.12 | 2.44 | 2.55 |
| 28 | 0.3 | 1 | 1 | 0.3 | 5.71 | 4.65 | 30.12 | 32.12 | 2.05 | 2.14 |
| 29 | 0.5 | 1 | 1 | 0.2 | 7.48 | 6.54 | 102.48 | 105.46 | 2.09 | 3.19 |

RSM model analysis

The primary model simulation was on basis of the analysis of variance (ANOVA) that gives quantitative data about the value of p. Here, ANOVA analysis related to various response parameters for example: Smooth load (W_S) /Rough load (W_R), Smooth friction (F_S) /Rough friction (F_R), Smooth flow-in (Q_S)/Rough flow-in (Q_R) were presented in table 2. Such method adjudged to be indifferent as the values of p were 0.05.

Evaluation of the RSM model

The sustainability of the model was compared through analysis of variance (ANOVA) given in table 3. For different responses, computed output proved the model to be important with p values lower than 10^{-4} . The initial value of p set as 0.005 [11]. The regression statistics such as goodness of fit (R^2) and the goodness of prediction (Adjusted R^2) were presented in table 3 related to all the

responses. As given in table 4, R^2 value shows the total variation of response when significant factors were considered. The Adjusted R^2 value decides the number of predictors of the simulation. Both values indicated in the simulation, converged very well to the data.

Fig.5 (a-f) show the variation of W_R over $\beta \sim \epsilon$, $G \sim \epsilon$, $Y \sim \epsilon$, $G \sim \beta$, $Y \sim \beta$, $Y \sim G$ surface representation respectively with double parameter influence. It helps in identifying the maximum, minimum and targeted value of W_R .

Fig. 6 (a-f) show the variation of F_R over $\beta \sim \epsilon$, $G \sim \epsilon$, $Y \sim \epsilon$, $G \sim \beta$, $Y \sim \beta$, $Y \sim G$ surface representation respectively with double parameter influence. It helps in identifying the maximum, minimum and targeted value of F_R . Fig. 7 (a-f) show the variation of Q_R over $\beta \sim \epsilon$, $G \sim \epsilon$, $Y \sim \epsilon$, $G \sim \beta$, $Y \sim \beta$, $Y \sim G$ surface representation respectively with double parameter influence. It helps in identifying the maximum, minimum and targeted value of Q_R

Table 3. Summary of Result of DoE.

| Source | W_{is} (Quardratic Model) | | W_R (Quardratic Model) | | F_{is} (Quardratic Model) | | F_R (Quardratic Model) | | Q_{is} (Quardratic Model) | | Q_R (Quardratic Model) | |
|-------------------------|--------------------------------|---------|-----------------------------|---------|--------------------------------|---------|-----------------------------|---------|--------------------------------|---------|-----------------------------|---------|
| | F | p-value | F | p-value | F | p-value | F | p-value | F | p-value | F | p-value |
| Model | 23.89 | <0.0001 | 6.42 | 0.0007 | 4.56 | 0.0038 | 2.56 | 0.0448 | 6.41 | 0.0007 | 6.46 | 0.0006 |
| ϵ | 127.82 | <0.0001 | 29.94 | <0.0001 | 2.96 | 0.1073 | 0.3184 | 0.5815 | 0.2257 | 0.6421 | 0.2115 | 0.6526 |
| β | 13.72 | 0.0024 | 1.40 | 0.2564 | 0.0288 | 0.8677 | 0.0077 | 0.9313 | 50.12 | <0.0001 | 61.33 | <0.0001 |
| G | 48.90 | <0.0001 | 10.96 | 0.0052 | 0.4211 | 0.5269 | 0.3841 | 0.5454 | 4.71 | 0.0477 | 0.1760 | 0.6812 |
| Y | 0.0302 | 0.8645 | 0.4833 | 0.4983 | 37.29 | <0.0001 | 17.24 | 0.0010 | 4.99 | 0.0424 | 2.57 | 0.1315 |
| $\epsilon \times \beta$ | 0.6335 | 0.4394 | 0.0030 | 0.9573 | 0.0001 | 0.9926 | 0.2243 | 0.6431 | 0.1067 | 0.7488 | 2.59 | 0.1296 |
| $\epsilon \times G$ | 21.29 | 0.0004 | 8.38 | 0.0118 | 0.0102 | 0.9211 | 0.0244 | 0.8782 | 0.5534 | 0.4692 | 0.4046 | 0.5350 |
| $\epsilon \times Y$ | 0.0266 | 0.8727 | 1.11 | 0.3104 | 1.64 | 0.2217 | 2.99 | 0.1056 | 0.0087 | 0.9271 | 0.7038 | 0.4156 |
| $\beta \times G$ | 0.7856 | 0.3904 | 1.95 | 0.1844 | 0.1584 | 0.6966 | 0.2388 | 0.6327 | 0.6054 | 0.4495 | 1.73 | 0.2094 |
| $\beta \times Y$ | 0.0049 | 0.9450 | 0.0210 | 0.8869 | 0.0286 | 0.8682 | 0.1679 | 0.6881 | 12.56 | 0.0032 | 6.28 | 0.0252 |
| $G \times Y$ | 0.0108 | 0.9186 | 1.172E-07 | 0.9997 | 1.90 | 0.1895 | 2.07 | 0.1717 | 0.0777 | 0.7845 | 0.1975 | 0.6635 |
| ϵ^2 | 21.29 | 0.0004 | 6.90 | 0.0199 | 0.1645 | 0.6912 | 1.72 | 0.2110 | 0.2073 | 0.6559 | 3.33 | 0.0893 |
| β^2 | 3.72 | 0.0744 | 1.64 | 0.2211 | 0.7103 | 0.4135 | 0.1382 | 0.7156 | 18.51 | 0.0007 | 21.95 | 0.0004 |
| G^2 | 2.21 | 0.1596 | 0.9197 | 0.3538 | 1.32 | 0.2697 | 0.2397 | 0.6320 | 3.05 | 0.1024 | 0.2066 | 0.6564 |
| Y^2 | 0.3950 | 0.5398 | 0.0101 | 0.9215 | 12.49 | 0.0033 | 5.24 | 0.0381 | 2.11 | 0.1684 | 2.55 | 0.1327 |

Table 4 Results of various statistical tests for validation of developed response models.

| Model test criteria | W_{is} | W_R | F_{is} | F_R | Q_{is} | Q_R |
|---------------------|----------|---------|----------|---------|----------|---------|
| R^2 | 99.46 | 99.81 | 88.64 | 89.11 | 98.53 | 98.34 |
| Adj R^2 | 98.74 | 99.34 | 89.56 | 89.52 | 98.45 | 97.32 |
| Pred R^2 | 97.34 | 98.54 | 88.53 | 87.65 | 98.02 | 97.12 |
| P-value | <0.0001 | <0.0001 | <0.0001 | <0.0001 | <0.0001 | <0.0001 |
| AD P-value | 0.053 | 0.072 | 0.057 | 0.233 | 0.414 | 0.089 |

Based on the input, the quadratic method of the responses was created out of actual factors and are given in table 3. It consists of output parameters in the quadratic form for individual

parameters (ϵ , β , G, Y) and cross correlated parameters ($\epsilon \times \beta$; $\epsilon \times G$; $\epsilon \times Y$; $\beta \times G$; $\beta \times Y$; $G \times Y$) and quadratic correlation (ϵ^2 , β^2 , G^2 , Y^2).

The effectiveness of model has been performed by the help of R^2 value. When R^2 approaches to the value of unity, implying the response models have closely resembled the simulation data. In the present works, the R^2 values for W_R , F_R , Q_R are 99.81%, 89.11%, 98.34% respectively, which

reveals statistical significance of the simulation and the right fit for the evaluation model. Further, the adjusted R^2 values for W_R , F_R , Q_R are 99.34%, 89.52%, 97.32% respectively and the total range is described by their respective simulation process after observing the significant factors.

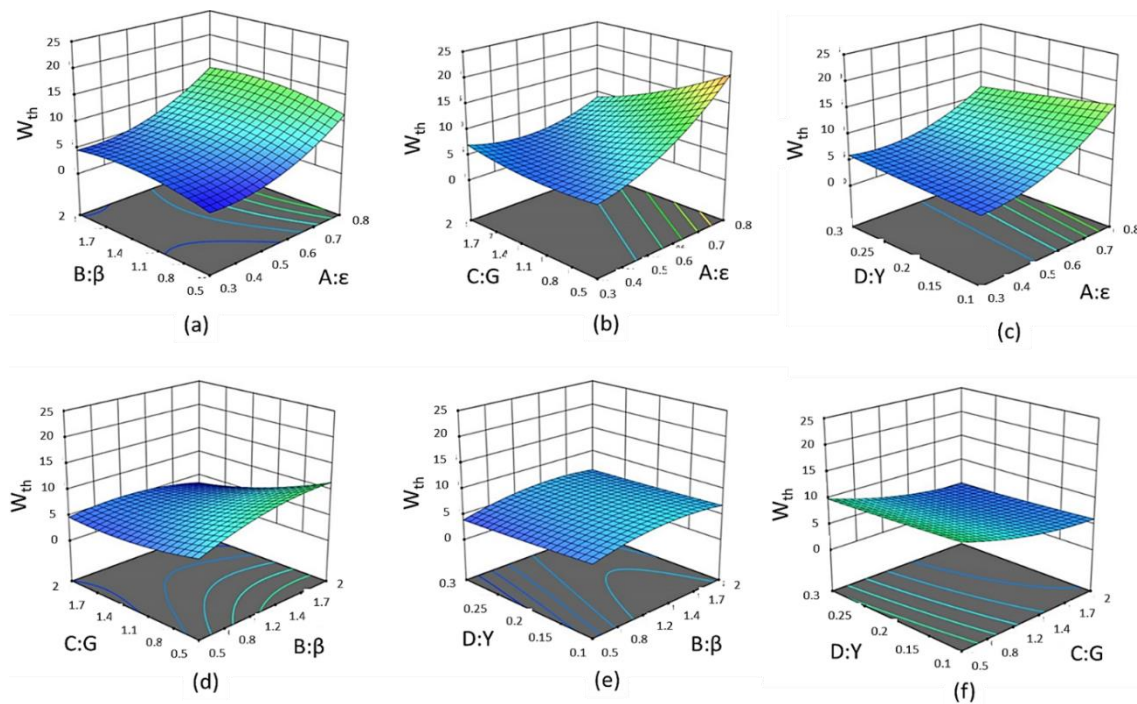


Fig. 5. W_R variation: (a) against L/D ratio (β) and eccentricities (ϵ); (b) against non-circularity (G) and eccentricities (ϵ); (c) against Roughness coefficient (Y) and eccentricities (ϵ); (d) against non-circularity (G) and L/D ratio (β); (e) against Roughness coefficient (Y) and L/D ratio (β); (f) against Roughness coefficient (Y) and non-circularity (G).

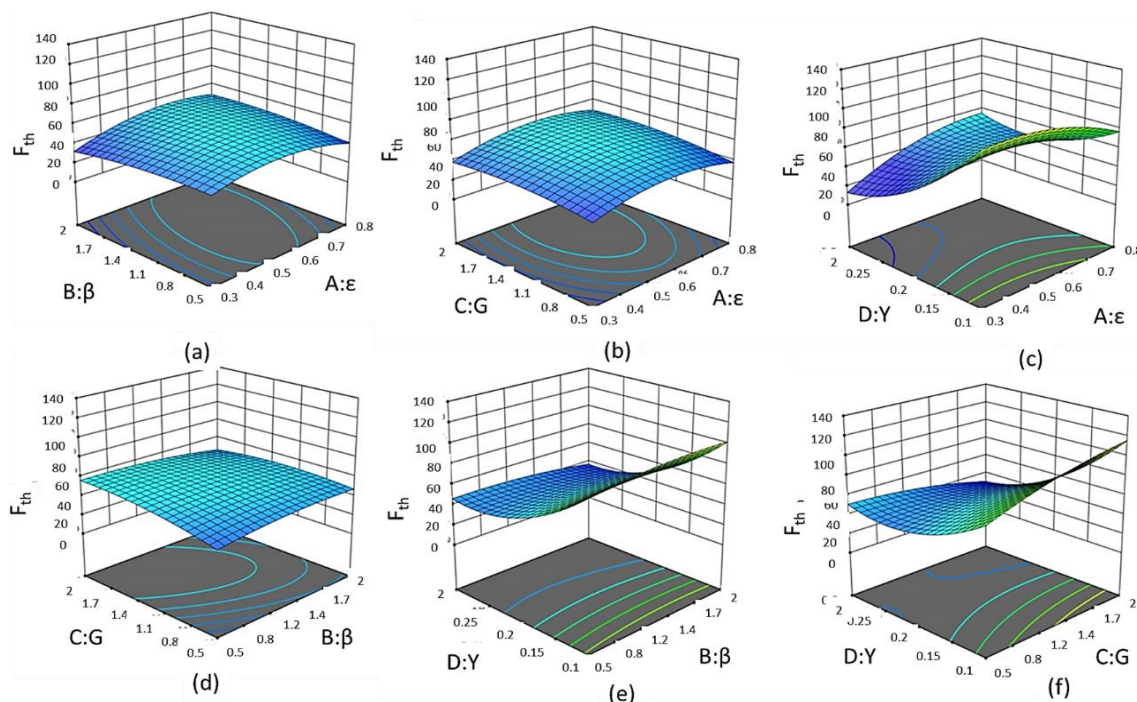


Fig. 6. F_R variations: (a) against L/D ratio (β) and eccentricities (ϵ); (b) against non-circularity (G) and eccentricities (ϵ); (c) against Roughness coefficient (Y) and eccentricities (ϵ); (d) against non-circularity (G) and L/D ratio (β); (e) against Roughness coefficient (Y) and L/D ratio (β); (f) against Roughness coefficient (Y) and non-circularity (G).

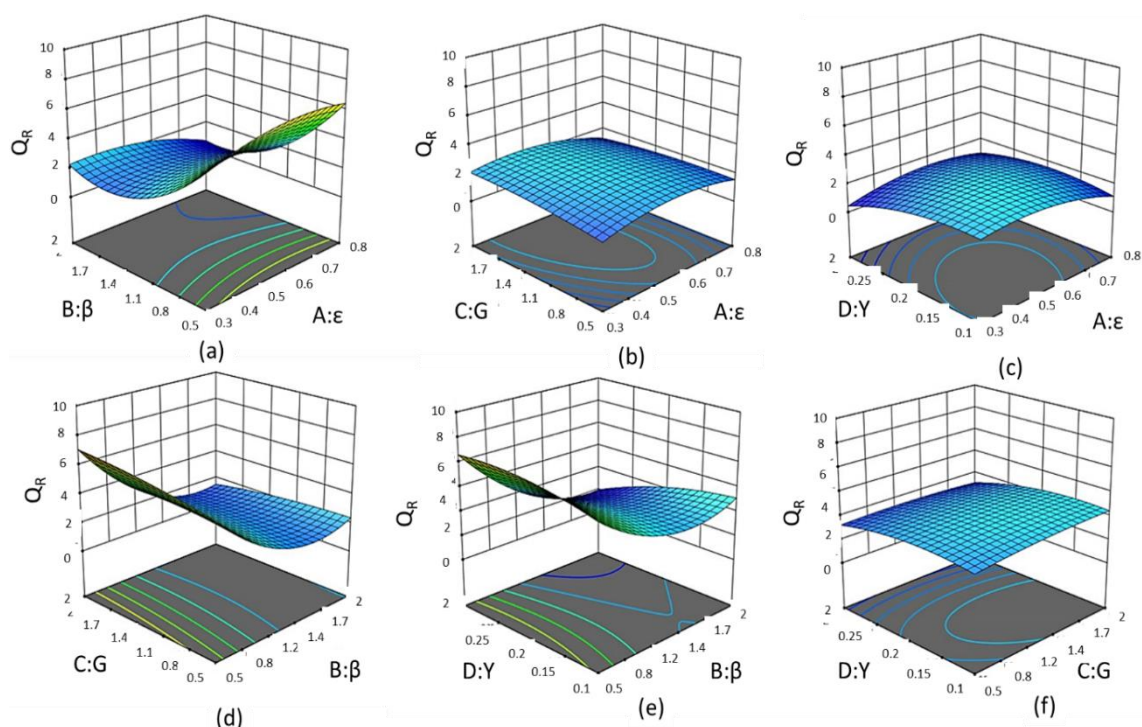


Fig. 7. Q_R variations: (a) against L/D ratio (β) and eccentricities (ϵ); (b) against non-circularity (G) and eccentricities (ϵ); (c) against Roughness coefficient (Y) and eccentricities (ϵ); (d) against non-circularity (G) and L/D ratio (β); (e) against Roughness coefficient (Y) and L/D ratio (β); (f) against Roughness coefficient (Y) and non-circularity (G).

4. CONCLUSION

The biggest advantage of a DOE analysis is that it provides a solution, and information about the space around that solution. This can lead to the researcher improving the design of the simulation, or changing an input parameter to improve the quality of the simulation. The following conclusions were done on performing the several simulations of rough elliptic bore journal bearing by varying the input parameters like eccentricities (ϵ), non-circularities (G), L/D ratio (β), roughness coefficient (Y).

- The Design of Experiments was most suitable in designing the simulation and the statistical analysis was useful in identifying the important responses that are highly influential to the hydrodynamic action of journal bearing. This simulation technique mostly minimizes the time involved in reducing the number of experiments to minimum due to which, it is capable of performing and facilitating statistically approved models for total response.

- Long journal bearing with more than non-circularity ($G=0.5$) not recommended for load carrying capacity point of view.
- At same roughness coefficient, bearing with higher non-circularity has more friction force due to fluid layer interaction.
- At the non-circularity of ($G=1.0$), the highest value of non-dimensional friction force is 142 at roughness coefficient of ($Y=0.1$).
- With increasing roughness coefficient, the oil flow decreases until ($Y=0.2$). There after it remains almost constant.

Now this is a specifically marked study, which is restricted to the numerical modelling related rough elliptic bore journal bearing. The immediate implication of this work is to upgrade the bearing design charts which are most widely used in Lubrication Industries. The limitation of the work is that it is missing experimental test for non-circular bearing performance measurement, which is the future research plan of the paper.

REFERENCES

[1] W.A. Crosby, *An Investigation of Performance of Journal Bearings with slightly irregular bore*, Tribology International, vol. 25, iss. 3, pp. 199-204, 1992, doi: [10.1016/0301-679X\(92\)90049-S](https://doi.org/10.1016/0301-679X(92)90049-S)

[2] P.C. Mishra, *Thermal Analysis of Elliptic Bore Journal Bearing*, Tribology Transactions, vol. 50, iss. 1, pp. 137-143, 2007, doi: [10.1080/10402000601105573](https://doi.org/10.1080/10402000601105573)

[3] H. Christensen, K. Tonder, *The Hydrodynamic lubrication of Rough Journal Bearings*, Journal of Tribology, vol. 72, iss. 1, pp. 166-172, 1973 doi: [10.1115/1.3451759](https://doi.org/10.1115/1.3451759)

[4] H. Christensen, *Stochastic Models for Hydrodynamic Lubrication of Rough Surfaces*, Proceedings of the Institution of Mechanical Engineers, vol. 184, pp. 1013-1025, 1969, doi: [10.1243/PIME_PROC_1969_184_074_02](https://doi.org/10.1243/PIME_PROC_1969_184_074_02)

[5] P.C. Mishra, *Analysis of rough elliptic bore journal bearing using expectancy model of surface roughness*, Tribology in Industry, vol. 36, no. 2, pp. 211-219. 2014

[6] D. Dowson, G.R. Higginson, *Elastohydrodynamic Lubrication: The Fundamentals of Roller and Gear Lubrication*, Pergamon, Oxford, UK, 1966.

[7] P.C. Mishra, *Thermal analysis of elliptic bore journal bearing considering shaft Misalignment*, Tribology Online, vol. 6, iss. 5, pp. 239-246, 2011, doi: [10.2474/trol.6.239](https://doi.org/10.2474/trol.6.239)

[8] P.C. Mishra, *Computer Simulation and Optimization of Elliptic Bore Journal Bearing*, Tribology in Industry, vol. 44, no. 1, pp. 322-333, 2022, doi: [10.24874/ti.1179.09.21.01](https://doi.org/10.24874/ti.1179.09.21.01)

[9] S.K. Pradhan, R. Kumar, P.C. Mishra, *Grey-Fuzzy Hybrid Optimization for Thermohydrodynamic Performance Prediction of Misaligned Rough Elliptic Bore Journal Bearing*, Lubricants, vol. 10, iss. 10, pp. 1-21, 2022, doi: [10.3390/lubricants10100274](https://doi.org/10.3390/lubricants10100274)

[10] S.K. Pradhan, P. Mishra, P.C. Mishra, *Application of artificial neural network for lubrication performance evaluation of rough elliptic bore journal bearing*, Journal of Computational Design and Engineering, vol. 9, iss. 2, pp. 279-295, 2022, doi: [10.1093/jcde/qwab004](https://doi.org/10.1093/jcde/qwab004)

[11] M. Pandian, S.P. Sivapirakasam, M. Udayakumar, *Investigation on the effect of injection system parameters on performance and emission characteristics of a twin cylinder compression ignition direct injection engine fuelled with pongamia biodiesel–diesel blend ing response surface methodology*, Applied Energy, vol. 88, iss. 8, pp. 2663–2676, 2011, doi: [10.1016/j.apenergy.2011.01.069](https://doi.org/10.1016/j.apenergy.2011.01.069)

[12] D.I. Ahmed, S. Kasolang, B.A. Khidhir, N.R. Abdullah, *Application of Response Surface Methodology to Predict Oil-Film Friction in Journal Bearing*, Applied Mechanics and Materials, vol. 393, pp. 931-937, 2013, doi: [10.4028/www.scientific.net/AMM.393.931](https://doi.org/10.4028/www.scientific.net/AMM.393.931)

[13] T. Lee, R.D. Reitz, *Response surface method optimization of a high-speed direct injection diesel engine equipped with a common rail injection system*, Journal of Engineering for Gas Turbines and Power, vol 145, iss. 3, pp. 541-546, 2003, doi: [10.1115/1.1559900](https://doi.org/10.1115/1.1559900)

[14] Y. Zhang, G. Chen, L. Wang, *A Calculation Method for the Journal Bearing with a Determined Load Based on Response Surface Optimization*. Tribology Transactions, vol. 63, iss. 4, pp. 647-657, 2020, doi: [10.1080/10402004.2020.1731037](https://doi.org/10.1080/10402004.2020.1731037)

[15] P.K. Kankar, S.P. Harsha, P. Kumar, S.C. Sharm, *Fault diagnosis of a rotor bearing system using response surface method*, European Journal of Mechanics – A/Solids, vol. 28, iss. 4, pp. 841-857, 2009, doi: [10.1016/j.euromechsol.2009.03.004](https://doi.org/10.1016/j.euromechsol.2009.03.004)

[16] H.P. Mishra, A. Jalan, *Analysis of faults in rotor-bearing system using three-level full factorial design and response surface methodology*, Noise & Vibration Worldwide, vol. 52, iss. 11, 2021, doi: [10.1177/09574565211030711](https://doi.org/10.1177/09574565211030711)

NOMENCLATURE

| | | | |
|-----------------|---|--------------|---|
| H | - Non-dimensional film | x, y, z | - Coordinates |
| G | - Ellipticity | τ | - Shear stress in fluid |
| θ | - Circumferential location | F_R | - Non-dimensional friction of rough bearing |
| $g_{1,2,3,4,5}$ | - Expectancy operators | q_θ^* | - Flow-in intensity |
| η | - Viscosity | Q | - Total flow-in |
| u | - Sliding velocity | d | - Desirability function |
| W_R | - Non-dimensional load of rough bearing | RSM | - Response surface methodology |
| Y | - Roughness coefficient | D | - Desirability function |
| ε | - Eccentricities ratio | DoE | - Design of experiments |
| β | - L/D ratio | | |